Biomedicine & Pharmacotherapy 139 (2021) 111566

Contents lists available at ScienceDirect

Biomedicine & Pharmacotherapy

journal homepage: www.elsevier.com/locate/biopha

Original article

Fe3O4@piroctone olamine magnetic nanoparticles: Synthesize and therapeutic potential in cutaneous leishmaniasis

Aishah E. Albalawi [a], Amal Khudair Khalaf [b], Mohamed S. Alyousif [c], Abdullah D. Alanazi [d,e], Parastoo Baharvand [f], Mojtaba Shakibaie [g], Hossein Mahmoudvand [h,*]

[a] Faculty of Science, University of Tabuk, Tabuk, Saudi Arabia
[b] Department of Microbiology, College of Medicine, University of Thiqar, Thiqar, Iraq
[c] Department of Zoology, College of Science, King Saud University, P.O. Box 2455, Riyadh 11451, Saudi Arabia
[d] Department of Biological Science, Faculty of Science and Humanities, Shaqra University, P.O. Box 1040, Ad-Dawadimi 11911, Saudi Arabia
[e] Alghad International Colleges for Applied Medical Science, Tabuk 47913, Saudi Arabia
[f] Department of Community Medicine, Lorestan University of Medical Sciences, Khorramabad, Iran
[g] Pharmaceutics Research Center, Institute of Neuropharmacology, Kerman University of Medical Sciences, Kerman, Iran
[h] Razi Herbal Medicines Research Center, Lorestan University of Medical Sciences, Khorramabad, Iran

ARTICLE INFO

Keywords:
Leishmania major
In vitro
In vivo
Amastigote
Nitric oxide
Cytotoxicity

ABSTRACT

Background: In recent years, magnetic nanoparticles (NMP) as novel materials have been widely used for biomedical, diagnostic and therapeutic purposes like microbial infection therapy. The purpose of this study is to synthesize PO coated iron oxide magnetic nanoparticles (Fe3O4@PO NPs) and their anti-leishmanial effects *in vitro* and *in vivo* against cutaneous leishmaniasis.

Methods: Fe3O4 magnetic nanoparticles were synthesized by the coprecipitation of Fe2 + and Fe3 + ions and used as a nanocarrier for the production of Fe3O4@PO NPs. The in vitro antileishmanial effects of PO-coated Fe3O4 NPs and Fe3O4 NPs (10–200 μg/mL) was determined against the intracellular amastigotes of *Leishmania major* (MRHO/IR/75/ER) and, then, examined on cutaneous leishmaniasis induced in male BALB/c mice by *L. major*. The rate of infectivity, production of nitric oxide (NO), and cytotoxic activates of Fe3O4 NPs and Fe3O4@PO NPs on J774-A1 macrophage cells were determined.

Results: The size scattering of the Fe3O4 NPs and Fe3O4@PO NPs were in the range among 1–40 and 5–55 nm, respectively. The obtained IC_{50} values were 62.3 ± 2.15 μg/mL, 31.3 ± 2.26 μg/mL, and 52.6 ± 2.15 μg/mL for the Fe3O4 NPs and Fe3O4@PO NPs, and MA, respectively. The results revealed that the mean number of parasites and the mean diameter of the lesions was considerably ($p < 0.05$) decreased in the infected mice treated with Fe3O4 NPs and Fe3O4@PO NPs. The Fe3O4 NPs and Fe3O4@PO NPs significantly ($p < 0.05$) prompted the production of NO as a dose-dependent manner. The promastigotes pre-incubated in Fe3O4 NPs and Fe3O4@PO NPs at the concentration of 5 μg/mL had the ability to infect only 41.7% and 28.3% of the macrophages cells. The selectivity index of greater than 10 for Fe3O4 NPs and Fe3O4@PO NPs showed its safety to the J774-A1 macrophage cells and specificity to the parasite.

Conclusion: The results of this survey indicated the high potency of Fe3O4@PO NPs to inhibit the growth of amastigote forms of *L. major* as well as recovery and improvement CL induced by *L. major* in BALB/c mice without significant cytotoxicity. The results also indicated that, although the possible anti-leishmanial mechanisms of Fe3O4@PO NPs have not been clearly understood, however, the triggering of NO may be considered as one of the possible anti-leishmanial mechanisms of these nanoparticles. However, additional studies, in particular in clinical contexts, are mandatory.

* Corresponding author.
E-mail address: dmahmodvand@gmail.com (H. Mahmoudvand).

https://doi.org/10.1016/j.biopha.2021.111566
Received 20 January 2021; Received in revised form 25 March 2021; Accepted 31 March 2021
Available online 8 April 2021

1. Introduction

Leishmaniasis is one of the major tropical/sub-tropical diseases caused by an intracellular parasite of the genus *Leishmania*. [1]. The disease characterizes a serious global health concern that represents a broad range of clinical features with a possibly fatal result [2]. The disease is classified into four clinical signs, including visceral leishmaniasis (VL), cutaneous leishmaniasis (CL), diffuse cutaneous leishmaniasis (DFL), mucocutaneous leishmaniasis (mL) [3,4]. According to the WHO reports, CL as the most prevalent form of leishmaniasis is divided into two main classes: (i) Old World *Leishmania* caused by L. *major* and L. *tropica* (the most prevalent species in the Middle East, Africa, and the Indian subcontinent); (ii) New World *Leishmania* caused by *L. amazonensis*, *L. mexicana*, *L. braziliensis*, etc (the most common in Middle and South Americas) [5,6].

Since a successful vaccine with high protection from all forms of leishmaniasis is not yet available, the choice of a suitable treatment strategy is therefore one of the best ways to interrupt the transmission cycle of the parasite and prevent the disease. [7]. Currently, a number of local and systemic therapeutic approaches exist for leishmaniasis, including physical approaches (e.g., surgery, laser therapy and cryotherapy) and chemical therapies [8]. Given existing chemical and synthetic drugs, past reports have shown that pentavalent antimonials (e.g., sodium stibogluconate (pentostame) and meglumine antimoniate (MA, glucantime) and second-line drugs because of certain limitations, such as treatment failure, the emergence of drug resistance, and reported side effects that pose serious problems in the treatment of CL [9,10]. As a result, improving and upgrading existing drugs, using new strategies such as combined therapy and nanomedicine as well as new and alternative drug discovery are the best strategies for managing and controlling CL. [11].

Over the past few days, the magnetic nanoparticles (MNPs) as novel materials have been broadly used for biomedical, diagnostic, and therapeutic purposes [12]. Among the magnetic NPs, iron oxide (Fe_3O_4) magnetic nanoparticles due to having high potency in site-specific delivery of the antimicrobials are broadly used as an antimicrobial delivery system to the infected sites [13]. In addition, these nanoparticles demonstrate high antimicrobial activity as a result of the use of components in their construction without the addition of antibiotics [14,15]. Previous studies have shown the antimicrobial activities of Fe3O4 MNPs against some bacterial, fungal, and parasitic strains including *Enterococcus hirae*, *Escherichia coli*, *Candida* spp, and *L. major* [16–18].

Piroctone olamine (PO), as an ethanolamine salt (1-hydroxy-4-methyl-6-(2,4,4-trimethylpentyl)− 2(1H)-pyridone) has been widely used in the preparation of cosmetic products especially in the dandruff treatment and fungal infections [19]. It has been shown that PO represents its antifungal activity by penetrating the cell membrane of fungi and subsequently inhibiting their energetic metabolism and oxygen absorption [19]. Previous studies have shown the apoptotic activity of PO on human and murine myeloma and lymphoma cell lines and its cytotoxic activity against the human fibrosarcoma cell line (HT-1080) [20].

Considering the biological and antimicrobial activity of Fe3O4 MNPs and PO, the purpose of this study is to synthesize PO coated iron oxide magnetic nanoparticles (Fe3O4@PO NPs) and their anti-leishmanial effects *in vitro* and *in vivo* against CL.

2. Materials and methods

2.1. Ethical statement

This study was reviewed and approved by the Ethics Committee of the Department of Biological Sciences at Shaqra University, Shaqra, Saudi Arabia (SH18-2020).

2.2. Synthesis of Fe3O4 NPs

The synthesis of Fe3O4 NPs performed using the technique of the alkalization of an aqueous solution containing Fe2 + and Fe3 + ions in a deoxygenated condition [21]. Initially, the reaction medium was deoxygenated using nitrogen gas for 60 min, and the FeSO4·4H2O (0.25 g/100 mL, Merck- Germany) along with FeCl3·6H2O (0.48 g/100 mL, Merck- Germany) were mixed in the deoxygenated deionized water by means of a magnet stirrer in 1000 rpm for 3 min. In the next step, 0.025 L of sodium hydroxide solution (0.29 M) was poured into the solution and was again stirred at 1000 rpm. The obtained sediment containing Fe3O4 NPs were washed several times with deoxygenated deionized water for 10 min at 80 °C. Finally, the obtained NPs were separated by a magnet and were lyophilized through a freeze dryer (FD-81; Eyela, Tokyo, Japan) and kept at 4 °C until testing.

2.3. Preparation of Fe3O4@PO NPs

Here, the precipitation approach was used for coating Fe3O4 MNPs by PO. Initially, A suspension of Fe3O4 NPs was provided using dissolving 0.1 g Fe3O4 NPs in 0.1 L of deionized water by means of ultrasonication (100 W) for 10 min. Then, 2 mL of chloroform solution of PO (30 mg/mL, Sigma–Aldrich, USA) was gently added to the Fe3O4 NPs solution for 5 min as continuous stirring (300 rpm) by a magnetic stirrer. In the next step, the obtained mixture was kept at 45 °C for 20 min and then the PO-coated Fe3O4 NPs were separated from the mixture by means of a magnet. After washing the obtained NPs with deionized water they were lyophilized and kept at 4 °C until testing.

2.4. Characterization of the NPs

The characterization of magnetic NP before and after the coating process was carried out using transmission electron microscopy (TEM). To do this, an aqueous suspension containing the NPs was added on carbon-coated copper TEM grids and dried below an infrared lamp. By a TEM equipment (Zeiss 902A, South Jena, Germany) micrographs was obtained operated at voltage of 80 kV. The particle size of the obtained NPs was determined through laser light scattering technique by means of a Zetasizer MS2000 (Malvern Instruments, Malvern, UK). The information of X-ray diffraction (XRD) of the resulting NPs was obtained on a P3000 diffractometer tool (Rich Seifert, NY, USA) using Cu-Kα radiation at a voltage of 40 kV and a current of 30 mA. A vibrating model magnetometer (Lakeshore, Westerville, OH, USA, 7307) was applied to evaluate the magnetic properties of Fe3O4 and Fe3O4@PO NPs at room temperature.

2.4.1. Fourier transform infrared spectroscopy

The dried magnetic NPs before and after the coating process, as well as PO, were used for Fourier transform infrared (FTIR) spectroscopy analysis using a PerkinElmer (Wellesley, MA, USA) Spectrum One tool under the resolution of 4 cm^{-1} in the potassium bromide (KBr) pellets.

2.4.2. UV-Vis spectroscopy analysis

A spectrophotometric method was used to quantitatively analyze the coating process. In brief, the standard curve of PO was obtained through scheming the determining absorbance at 304 nm, by means of a UV–visible spectrophotometer (UVD-2950; Labomed, CA, USA). After adding the 0.2 g of the washed Fe3O4@PO NPs to ethyl alcohol (50 mL), the absorbance of separated Fe3O4 NPs was determined at 304 nm to assess the quantity of the PO coated on the NPs surface.

2.5. In vitro antileishmanial effects against L. major

2.5.1. Parasite and cell culture

Promastigotes of *L. major* (MRHO/IR/75/ER) were prepared and cultured in RPMI 1640 (Sigma-Aldrich) upgraded with heat-inactivated

fetal calf serum (FCS) (Sigma-Aldrich), streptomycin (100 μg/mL), and penicillin (200 IU/mL). After preparing the murine macrophage cell line of J774-A1 from Pasteur Institute, Iran they were cultured in Dulbecco's modified Eagle's medium (DMEM, Sigma-Aldrich) added with 10% FCS at 37 °C in 5% CO_2.

2.5.2. Anti-intracellular amastigote effects

The effects of PO-coated Fe3O4 NPs, Fe3O4 NPs, and MA against the anti-intracellular amastigotes were examined using the approaches previously performed [22]. At first, promastigotes of *L. major* (1×10^6/mL) in the stationary phase were incubated with the J774-A1 macrophages (1×10^5/mL) placed in eight-chamber LabTek tissue-culture slides as the ratio of 10 parasites to 1 macrophage and for 24 h. Parasites that did not adhere to the cells were removed by washing with RPMI 1640 medium, Then the infected macrophages were treated to different concentrations of PO-coated Fe3O4 NPs (10–200 μg/mL) and Fe3O4 NPs (10–200 μg/mL) and MA(10–200 μg/mL) at 37 °C in 5% CO_2 for 2 days. After this incubation period, all slides were fixed with methanol and stained with Giemsa stain for evaluation with a light microscope. Evaluation of anti-amastigote effects was determined as follows the calculating the mean number of amastigotes in each macrophage after detecting 100 macrophage cells compared with those in control groups. Non-treated infected macrophages and non-infected non-treated macrophages were considered as positive and negative controls, respectively. Moreover, by Probit test in SPSS software, the 50% inhibitory concentrations (IC_{50} values) for all the studied groups were calculated.

2.5.3. Plasma membrane permeability

The plasma membrane permeability of the promastigotes (1×10^6 cells/mL) treated with various concentrations of PO-coated Fe3O4 NPs and Fe3O4 NPs (50–200 μg/mL) was evaluated by Sytox green stain based on the manufacturer's instructions. Non-treated cells and cells with 2.5% of Triton X-100 (Sigma-Aldrich) were considered as the negative and positive control, respectively. Measurements were performed by using a microplate reader (BMG Labtech, Germany) every 60 min for 4 h.

2.5.4. Evaluating inhibition of infection in macrophage cells

Inhibitory effect of PO-coated Fe3O4 NPs and Fe3O4 NPs on infection in macrophage cells was assessed by pre-incubation of *L. major* promastigotes (10^6/mL) in PO-coated Fe3O4 NPs (5 μg/mL) and Fe3O4 NPs (5 μg/mL) for 2 h at 21 °C. After this time, the washed parasites were incubated in macrophage cells for 4 h. Finally, the slides were fixed by methanol, staining with Giemsa, and were tested with a light microscope to evaluate the inhibition of infection through calculating 100 macrophage cells [23].

2.5.5. Determining the nitric oxide (NO) production

Effect of PO-coated Fe3O4 NPs and Fe3O4 NPs on NO production was measured using Griess reaction technique [24]. For this goal, 0.1 mL of the supernatants of macrophages treated with PO-coated Fe3O4 NPs and Fe3O4 NPs for 72 h. Then the Griess reagent A and, then, 60 μL of Griess reagent B (60 μL from each) (A and B, Sigma-Aldrich) were placed into a 96-well culture plate containing the macrophages supernatants. Lastly, the production of NO was determined by reading the plates at 540 nm in an ELISA reader (BioTek-ELX800).

2.5.6. Cytotoxic effects of J774-A1 macrophage cells

Cytotoxic effects of PO-coated Fe3O4 NPs and Fe3O4 NPs on the J774-A1 normal cells was aimed by means of treating the cells (5×10^5) with various concentrations of PO-coated Fe3O4 NPs and Fe3O4 NPs (0–500 μg/mL) at 37 °C in 5% CO_2 for 48 h. The viability of J774-A1 cell was finally measured using the MTT ([3-(4.5-dimethylthiazol-2-yl)−2.5-diphenyl tetrazolium bromide)]) assay. The 50% cytotoxic concentrations (CC_{50} values) were also calculated using the Probit test in SPSS software. Besides, to judge toxicity and activity of nanoparticles, the selectivity index (SI) was exhibited based on the CC_{50} calculation for macrophages cells/IC_{50} for *L. major* amastigote forms [24].

2.6. In vivo antileishmanial effects against cutaneous leishmaniasis

2.6.1. Animal

Forty-eight male BALB/c mice with weighting 20–25 g and 6–8 weeks old were kept in a colony room with a 12 h/2 h light/dark cycle at 21 ± 2 °C. The mice were randomly divided into 6 groups (8 mice per group) included (i) infected mice treated with normal saline; (ii) infected mice treated with MA (30 mg/kg/day); (iii) infected mice treated with Fe3O4 NPs 1 mg/kg/day; (iv) infected mice treated with Fe3O4 NPs 2 mg/kg/day; (v) infected mice treated with Fe3O4@PO NPs 1 mg/kg/day; (vi) infected mice treated with Fe3O4@PO NPs 2 mg/kg/day.

2.6.2. Inducing cutaneous leishmaniasis in BALB/c mice

CL was established by subcutaneous inoculation of 0.1 mL of *L. major* promastigotes (2×10^6 parasites/mL) in the stationary phase at the base of the mice tail [25]. This investigation was done inconsistency with the recommendations of the Guide for Care and Use of Laboratory Animals of the National Institutes of Health.

2.6.3. Treating infected mice

Forty-two days after infection, once CL lesions observed, the treatment of infected mice was started. Then, various concentrations of PO-coated Fe3O4 NPs and Fe3O4 NPs (1 and 2 mg/kg) were used topically for each tested group once a day for 4 weeks. A Vernier caliper was used to measure the diameter of the CL lesions before and after the treatment. Animals in the control group received equivalent volumes of the vehicle as treatment animals (saline). The positive control group received MA (30 mg/kg) as the intralesional injection. In addition, the parasite load in the mice of each tested group was measured via impression smears obtained from the lesions. The smears were fixed by methanol and, then, staining them with Giemsa, they were examined with a light microscope to calculate the parasite load in each tested group [25].

2.7. Statistical analysis

All of the experiments were carried out in triplicate. SPSS statistical package, version 22.0 (SPSS, Inc.), was applied for data analysis. The unpaired samples *t*-test and one-way analysis of variance (ANOVA) followed by the Dunnett's test were used for comparisons between the groups. Results were expressed as mean ± standard deviation. Furthermore, $p < 0.05$ was considered statistically significant.

3. Results and discussion

3.1. Characterization of NPs

Morphological properties (shape and size) of synthesized nanoparticles before and after the coating procedure were studied by TEM (Fig. 1A and B). The size distribution of the Fe3O4 NPs and Fe3O4@PO NPs were in the range among 1–40 and 5–55 nm, respectively. Whereas the most common particles in Fe3O4 NPs and Fe3O4@PO NPs had the size of 10–15 and 15–20 nm, respectively. Accumulation among the NPs may be caused by the large surface area of the NPs and the magnetic forces among them [19]. Based on the findings, adding PO on the surface of the magnetic NPs increases the size of nanoparticles. In line with our results, Khorramizadeh et al. demonstrated that the coating of the magnetic NPs with other organic compounds such as umbelliprenin could increase the size of nanoparticles [21].

As shown in Fig. 1-C1, the pattern of XRD of Fe3O4@PO NPs with seven characteristic peaks of 2θ, 30.1°, 35.6°, 43.3°, 53.5°, 57°, 63°, and 74° approved that the magnetic Fe3O4@PO were properly synthesized; while the coating procedure by PO did not have an apparent effect on

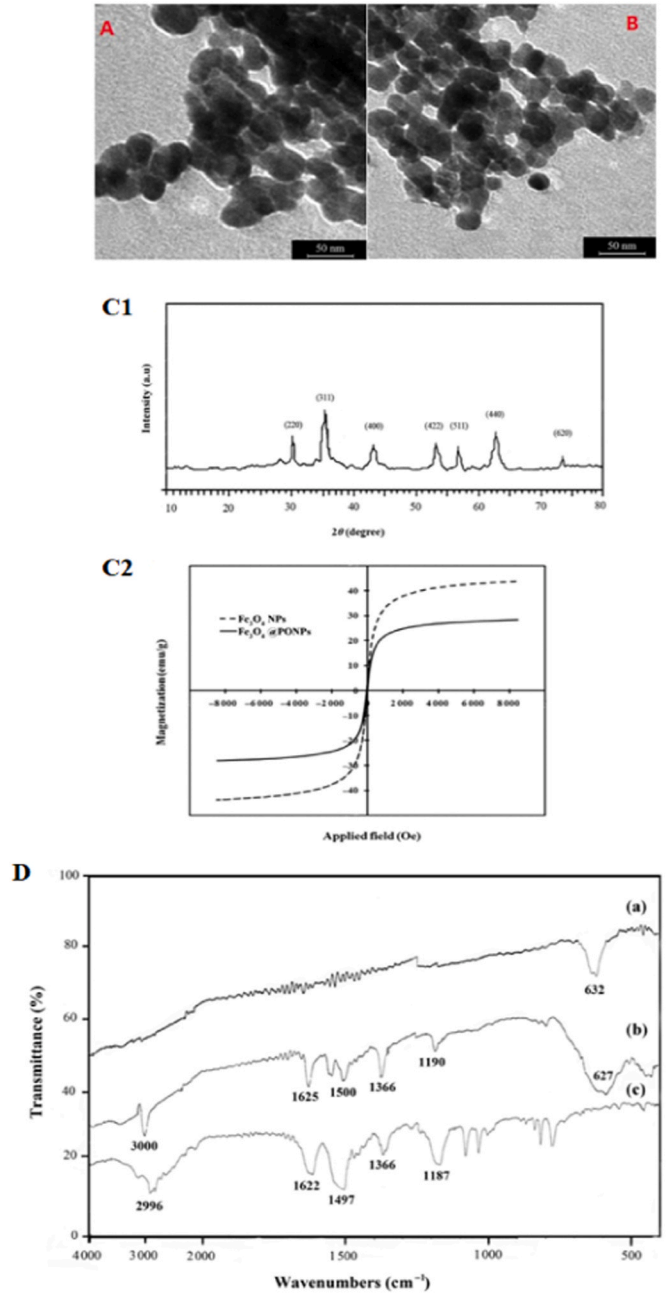

Fig. 1. Transmission electron microscope of chemically synthesized (A) Fe3O4@PO NPs and (B) Fe3O4 NPs. C1 shows X-ray diffraction pattern of Fe3O4@PO NPs with seven characteristic peaks of 2θ, 30.1°, 35.6°, 43.3°, 53.5°, 57°, 63°, and 74° approved that the magnetic Fe3O4@PO were properly synthesized; C2 shows magnetic hysteresis curves of Fe3O4 NPs and Fe3O4@PO NPs obtained at room temperature, indicated that the obtained Fe3O4 MNPs and Fe3O4@PO NPs have a clear ferromagnetic characterization. Fe3O4 and Fe3O4@PO NPs have saturation magnetization (MS) with values of 43.7 and 28.2 emu/g, respectively. D: FTIR spectrum of (a) Fe3O4 NPs, (b) Fe3O4@PO NPs, and (c) PO.

the crystalline structure of Fe3O4 MNPs. Consistent with our results, Gan et al. demonstrated that coating of Fe3O4 MNPs using boronic acid did not change the XRD pattern of Fe3O4 NPs [26].

Fig. 1-C2 displayed that the obtained Fe3O4 MNPs and Fe3O4@PO NPs have a clear ferromagnetic characterization. The obtained results showed that Fe3O4 and Fe3O4@PO NPs have saturation magnetization (MS) with values of 43.7 and 28.2 emu/g, respectively; while these values were lower than the bulk Fe3O4 with MS value of 90 emu/g. This reduction in MS values of nanoparticles can be attributed to the increase in the size of Fe3O4 NPs as well as the attendance of PO on the surface of these nanoparticles. In line with our findings, Wei et al. (2013), have reported that the change of Fe3O4 surface by means of oleic acid and sodium citrate results in a reduction in the MS [27].

We used the FTIR measurements to determine the functional groups placed on the surface of NPs (Fig. 1D). As shown in Fig. 4a, the Fe3O4 NPs exhibited the typical absorption of Fe–O bond at 632 cm^{-1}. Whereas, Fe3O4@PO NPs represents the key peaks at 3000, 1625, 1500, 1366, 1190, and 627 wave numbers (cm^{-1}) for O–H or N–H, C=O, C=C, C–N, C–O or C–N, and Fe–O functional groups, respectively. Fig. 4c demonstrated the similar high peaks in FTIR spectrum of PO (2996, 1622, 1497, 1366, and 1187 cm^{-1}); indicating that the coating process was performed properly.

3.2. *In vitro and in vivo antileishmanial effects*

The obtained results revealed that Fe3O4 NPs and Fe3O4@PO NPs significantly ($p < 0.001$) inhibited the growth rate of *L. major* amastigotes based on a dose-dependent response (Fig. 2A). The obtained IC_{50} values were 62.3 ± 2.15 μg/mL, 31.3 ± 2.26 μg/mL, and 52.6 ± 2.15 μg/mL for the Fe3O4 NPs and Fe3O4@PO NPs, and MA, respectively (Table 1).

As shown in Fig. 2B, the mean diameter of lesion size in the infected mice after 30 days of treatment in comparison with the control group. The mean diameter of the lesions after treatment of mice with the concentrations of 1 and 2 mg/mL of Fe3O4 NPs was decreased by 4.8 and 6.1 mm, respectively. The mean diameter of the lesions after treatment of mice with the concentrations of 1 and 2 mg/mL Fe3O4@PO NPs was decreased by 8.1 and 9.0 mm, respectively. However, in the untreated mice, the mean diameter of the lesions increased by 8.2 mm. The results also revealed that the mean number of parasites was considerably ($p < 0.05$) decreased in the infected mice treated with NPs especially Fe3O4@PO NPs (Fig. 2C). The mean number of parasites in control group was 2.66×10^3. This value for mice treated with Fe3O4 NPs at the doses of 1 and 2 mg/kg was 1.11×10^3 and 0.81×10^3, respectively; whereas the mean number of parasites in mice treated with Fe3O4@PO NPs at the doses of 1 and 2 mg/kg was 0.61×10^3 and 0.39×10^3, respectively.

Today, the new drug delivery systems are considered valuable approaches to reduce the limitations linked with the existing medication strategies. In recent years, the treatment of leishmaniasis represents various limitations because of the toxicity and adverse side effects of first-line agents. Recently, Nafari et al. have demonstrated that some drug carriers such as nanoparticles are able to support reducing toxicity and improving the efficacy of the leishmaniasis agents. They also reported that polymeric, liposome, lipid nanoparticles, as well as some metal oxides nanoparticles (e.g. Zinc oxide, Titanium dioxide, Silver dioxide) as new agents for the treatment of leishmaniasis [28]. Nowadays, the FeO nanoparticles due to having some unique properties such as easy sequestration by the spleen and finally removed by the cells of the phagocyte system, have broadly been suggested as an exceptional agent to drug delivery systems [29].

Considering the antiparasitic effects of iron oxide (FeO) nanoparticles, previously Khatami et al. have demonstrated that Fe3O4 nanoparticles had the antileishmanial effects on the *L. major* promastigotes as on a dose-dependent manner with the IC_{50} value of 350 μg/mL [17]. Dorostkar et al. have demonstrated that the FeO nanoparticles at the doses of 0.004%, 0.008%, and 0.012% w/v significantly reduced the mobility as well as the increased mortality rate of *Toxocara vitulorum in vitro* [30]. Kannan et al. (2019) have evaluated the antimalarial effects of iron oxide nanoparticle fortified artesunate against wild type andartemisinin-resistant *Plasmodium falciparum* (R539T) grown in O+ ve human blood and in *P. berghei* ANKA infected swiss albino mice, the results showed that the FeO nanoparticles fortified artesunate had potent antiparasitic effects at the concentration of 0.4 nM, so that

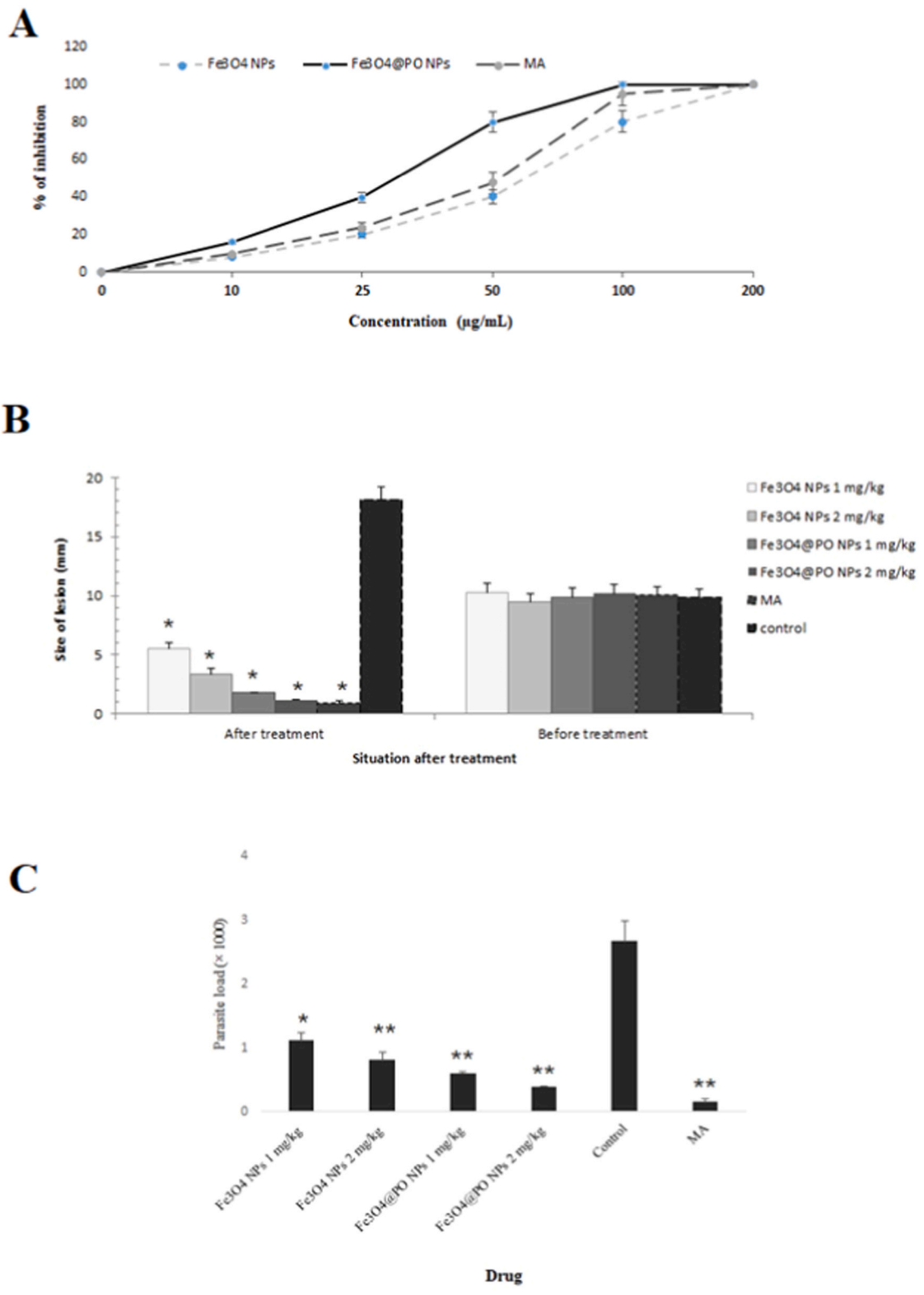

Fig. 2. The obtained results revealed that Fe3O4 NPs and Fe3O4@PO NPs significantly ($p < 0.001$) inhibited the growth rate of L. *major* amastigotes based on a dose-dependent response. The obtained IC_{50} values were 62.3 ± 2.15 µg/mL, 31.3 ± 2.26 µg/mL, and 52.6 ± 2.15 µg/mL for the Fe3O4 NPs and Fe3O4@PO NPs, and MA, respectively (A). Antileishmanial effects of Fe3O4 NPs, Fe3O4@PO NPs, and MA on the size of lesions in BALB/c mice infected by *L. major*. * $P < 0.001$ (B). Comparison of mean number of parasites (parasite load) in infected mice after treatment with various concentrations of Fe3O4 NPs, Fe3O4@PO NPs, and MA compared with control group. * $P < 0.05$; ** $P < 0.001$ (C).

Table 1
The IC_{50} and CC_{50} values (μg/mL) determined for the Fe3O4 NPs and Fe3O4@PO NPs, compared with the MA and their selectivity index (SI) against intramacrophage amastigote forms of *Leishmania major*.

Tested material	IC_{50} (μg/mL) for L. *major* amastigote	CC_{50} (μg/mL) of the J774-A1 cells	SI
Fe3O4 NPs	62.3 ± 2.15	645.25 ± 9.15	10.36
Fe3O4@PO NPs	31.3 ± 2.26	358.3 ± 7.63	11.43
MA	52.6 ± 2.15	1125.6 ± 11.60	21.39

Table 2
Inhibition of the infection in macrophage cells after treatment of *L. major* promastigotes with the Fe3O4 NPs and Fe3O4@PO NPs. Data are expressed as the mean ± SD (n = 3).

Promastigotes	Percentage of infected macrophages	Infectiveness reduction (%)
Non-treated	81.3 ± 3.15	–
Treated with Fe3O4 NPs (5 μg/mL)	41.7 ± 2.33	39.6
Treated with Fe3O4@PO NPs (5 μg/mL)	28.3 ± 2.46	53.0

inhibited the growth of *P. falciparum* with considerable damage to macromolecules mediated through increased reactive oxygen species (ROS) production. They also reported that artesunate fortified with iron oxide nanoparticles significantly reduced the parasitemia between 8 and 10-fold compared with artesunate alone in infected mice with *P. berghei* [31].

Since inhibiting the growth of intracellular organisms is characterized by rupture and/or cross plasma membrane, we evaluated the plasma membrane integrity of the treated of the promastigotes. The results of relative fuorescent units (RFU) demonstrated that the promastigotes treated with Fe3O4 NPs and Fe3O4@PO NPs especially at the concentration of 200 μg/mL alter the plasma membrane integrity by Sytox Green (Fig. 3); whereas positive control (Triton X-100) permeabilized cells with increase in detected fuorescence. Previously, Zanella et al. (2017) have demonstrated that the possibility of cytomembranes being permeable to uncoated FeNPs. The also demonstrated that FeNPs through crossing lipid bilayers enter cytoplasm and other cellular compartments [32]. At present, infectivity is considered as one of the main pathogenic and biological factors of *Leishmania* parasites [23]. Here we evaluated the effects of PO-coated Fe3O4 NPs and Fe3O4 NPs on the infectivity rate of *L. major* promastigotes. The results revealed that *L. major* promastigotes which were not pre-incubated with nanoparticles were able to infect 81.3% of the macrophage cells, while the promastigotes pre-incubated in Fe3O4 NPs and Fe3O4@PO NPs at the concentration of 5 μg/mL had the ability to infect only 41.7% and 28.3% of the J774-A1 macrophages cells (Table 2).

NO as an important product of macrophages is considered as one of the main mediators to eliminate intracellular parasites such as *Leishmania* [33]. We assessed the effect of PO-coated Fe3O4 NPs and Fe3O4 NPs on NO production using the Griess reaction for nitrites method. The obtained findings exhibited that the Fe3O4 NPs and Fe3O4@PO NPs significantly ($p < 0.05$) prompted the production of NO in a dose-dependent manner. Fig. 4 indicates the production of NO by Fe3O4 NPs and Fe3O4@PO NPs at the concentrations of 25 and 50 μg/mL compared to the non-treated macrophage cells. Consistent with our results, Dorostkar et al. have demonstrated that FeO nanoparticles

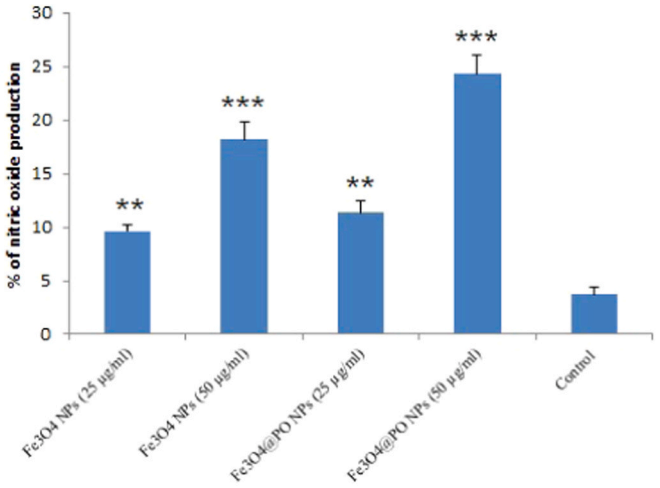

Fig. 4. Comparison of NO production in J774-A1 macrophage cells after treatment with various concentrations of the Fe3O4 NPs and Fe3O4@PO NPs using Griess reaction for nitrites. ** $P < 0.01$; *** $P < 0.001$.

significantly increased NO level, superoxide dismutase activity, and malondialdehyde activity as a time and dose-dependent response in a homogenized mixture of *T. vitulorum* adult worms [30]. De Lima et al. (2013) have also exhibited that NO- releasing iron oxide magnetic nanoparticles promote apoptosis and cell death compared to free NO-nanoparticles [34]. In the other study conducted by Seabra et al. (2012), it has been proven that iron oxide nanoparticles might be applied as proper vehicle to transport and delivery NO in biomedical uses, since the nanoparticles could be conducted to the target site under a magnetic field to delivery NO direct to the chosen target place [35]. These results suggest that although Fe3O4 NPs coated with PO and Fe3O4 NPs increased NO production as a key intracellular antimicrobial

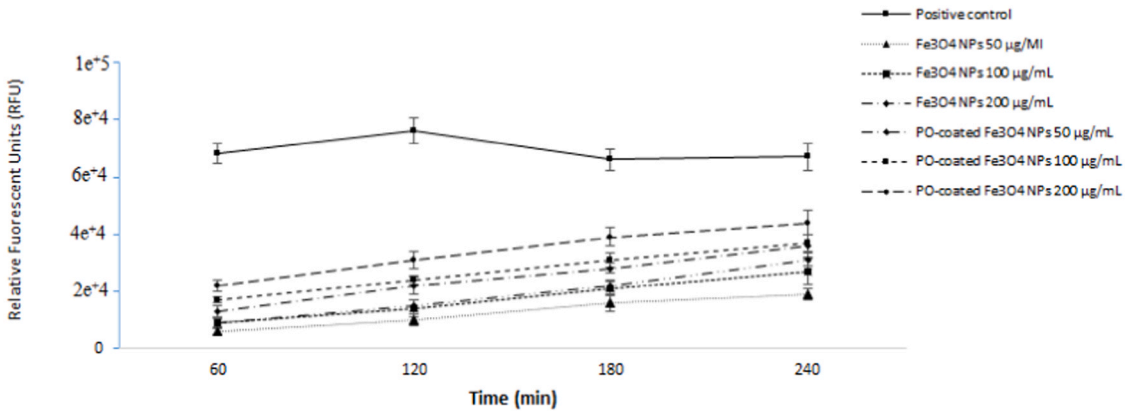

Fig. 3. The relative fuorescent units (RFU) for evaluation of the plasma membrane permeability of the promastigotes (10^6 cells/mL) treated with various concentrations of PO-coated Fe3O4 NPs and Fe3O4 NPs (50–200 μg/mL) was evaluated by Sytox green stain.

mechanism; however, further experiments and analyses are necessary to measure the significance of NO and exclude other factors.

Considering the antimicrobial effects of the piroctone olamine, do Couto et al. demonstrated that PO have potent antifungal effects against some *Candida* strains (e.g. *Candida albicans, C. parapsilosis, C. tropicalis, C. glabrata, C. guilliermondii, C. krusei*) with low minimum inhibitory concentrations (MICs) ranging from 0.125 to 0.5 μg/mL [36]. They also reported high in vivo anti-fungal activity in the fungal growth score in experimental intra-abdominal candidiasis [36].

With respect to the cytotoxicity effects of Fe3O4 NPs and Fe3O4@PO NPs, the obtained results of MTT assay revealed that Fe3O4 NPs and Fe3O4@PO NPs had no significant cytotoxicity in J774 cells. The CC_{50} value of the Fe3O4 NPs and Fe3O4@PO NPs was 645.25 and 358.3 μg/mL. The SI of greater than 10 for Fe3O4 NPs and Fe3O4@PO NPs showed its safety to the J774-A1 macrophage cells and specificity to the parasite (Table 1). Shakibaei et al. have reported that the cytotoxic effect of the Fe3O4@PO NPs is higher than Fe3O4 NPs; however, Fe3O4@PO NPs and Fe3O4 NPs nanoparticles at the concentration 120 μg/mL had no significant cytotoxicity against Hs68 normal cell line with the viability of 75% and 89%, respectively [20]. Recently, Zhang et al. have reported although magnetic Fe3O4 nanoparticles on the size 120 and 250 nm at the various concentrations of had no significant toxicity on chicken macrophage cells (HD11); however, the cytotoxicity of these nanoparticles increases with decreasing size [37]. Accordingly, the previous studies revealed that cytotoxicity effects of these nanoparticles were associated to their size, concentration, time, shape, and cell type [37–39].

4. Conclusion

The results of this survey indicated the high potency of Fe3O4@PO NPs to inhibit the growth of amastigote forms of *L. major* as well as recovery and improvement CL induced by *L. major* in BALB/c mice without significant cytotoxicity. The results also indicated that, although the possible anti-leishmanial mechanisms of Fe3O4@PO NPs have not been clearly understood, however, the triggering of NO may be considered as one of the possible anti-leishmanial mechanisms of these nanoparticles. However, additional studies, in particular in clinical contexts, are mandatory.

Funding

Not applicable.

Conflict of interest statement

The authors declare that they have no known competing financial interests or personal relationships that could have appeared to influence the work reported in this paper.

References

[1] E. Torres-Guerrero, M.R. Quintanilla-Cedillo, J. Ruiz-Esmenjaud, R. Arenas, Leishmaniasis: a review, F1000Research 6 (2017) 750.
[2] B.M. Scorza, E.M. Carvalho, M.E. Wilson, Cutaneous manifestations of human and murine leishmaniasis, Int. J. Mol. Sci. 18 (6) (2017) 1296, https://doi.org/10.3390/ijms18061296. PMID: 28629171; PMCID: PMC5486117.
[3] K. Bi, Y. Chen, S. Zhao, Y. Kuang, Wu.C.H. John, Current visceral leishmaniasis research: a research review to inspire future study, BioMed. Res. Int. 2018 (2018) 1–13, https://doi.org/10.1155/2018/9872095. PMID: 30105272; PMCID: PMC6076917.
[4] S. Burza, S.L. Croft, M. Boelaert, Leishmaniasis, Lancet 392 (10151) (2018) 951–970, https://doi.org/10.1016/S0140-6736(18)31204-2. Epub 2018 Aug 17. PMID: 30126638.
[5] WHO. Leishmaniases C. Control of the leishmaniases: Report of a meeting of the WHO Expert Commitee on the Control of Leishmaniases, March 22–26 2010. WHO Tech Rep Ser. Geneva: World Health Organization 2010:xii. PubMed PMID: 21485694.
[6] L. Stockdale, R. Newton, A review of preventative methods against human leishmaniasis infection, PLoS Negl Trop Dis 20 (7) (2013), e2278.
[7] J. Alvar, I.D. Vélez, C. Bern, M. Herrero, P. Desjeux, J. Cano, J. Jannin, M. Boer, Leishmaniasis worldwide and global estimates of its incidence, PLoS ONE 7 (5) (2012), e35671.
[8] B.S. Mcgwire, A.R. Satoskar, Leishmaniasis: clinical syndromes and treatment, QJM Int. J. Med. 107 (1) (2014) 7–14.
[9] L. Monzote, Current treatment of leishmaniasis: a review, Open Antimicrob. Agents J. 1 (1) (2009).
[10] D.O. Santos, C.E. Coutinho, M.F. Madeira, C.G. Bottino, R.T. Vieira, S. B. Nascimento, A. Bernardino, S.C. Bourguignon, S. Corte-Real, R.T. Pinho, C. R. Rodrigues, Leishmaniasis treatment—a challenge that remains: a review, Parasitol. Res. 103 (1) (2008) 1–10, 1-0.
[11] L.F. Oliveira, A.O. Schubach, M.M. Martins, S.L. Passos, R.V. Oliveira, M. C. Marzochi, C.A. Andrade, Systematic review of the adverse effects of cutaneous leishmaniasis treatment in the New World, Acta Trop. 118 (2) (2011) 87–96.
[12] A.E. Albalawi, A.D. Alanazi, P. Baharvand, M. Sepahvand, H. Mahmoudvand, High Potency of Organic and Inorganic Nanoparticles to Treat Cystic Echinococcosis: An Evidence-Based Review. Nanomaterials 10 (12) (2020), 2533.
[13] S. F Hasany, N. H Abdurahman, A. R Sunarti, R. Jose, Magnetic iron oxide nanoparticles: chemical synthesis and applications review, Curr. Nanosci. 9 (5) (2013) 561–575.
[14] S. F Hasany, N. H Abdurahman, A. R Sunarti, R. Jose, Magnetic iron oxide nanoparticles: chemical synthesis and applications review, Curr. Nanosci. 9 (5) (2013) 561–575.
[15] C. Xu, J. Zheng, A. Wu, Applications of iron oxide-based magnetic nanoparticles in the diagnosis and treatment of bacterial infections, Front. Bioeng. Biotechnol. 7 (2019) 141.
[16] L. Gabrielyan, A. Hovhannisyan, V. Gevorgyan, M. Ananyan, A. Trchounian, Antibacterial effects of iron oxide (Fe3O4) nanoparticles: distinguishing concentration-dependent effects with different bacterial cells growth and membrane-associated mechanisms, Appl. Microbiol. Biotechnol. 103 (6) (2019) 2773–2782, https://doi.org/10.1007/s00253-019-09653-x. Epub 2019 Feb 1. PMID: 30706116.
[17] M. Khatami, H. Alijani, I. Sharifi, F. Sharifi, S. Pourseyedi, S. Kharazi, M.A. Lima Nobre, M. Khatami, Leishmanicidal activity of biogenic Fe3O4 nanoparticles, Sci. Pharm. 85 (4) (2017) 36.
[18] N.S. Seddighi, S. Salari, A.R. Izadi, Evaluation of antifungal effect of iron-oxide nanoparticles against different Candida species, IET Nanobiotechnol. 11 (7) (2017) 883–888.
[19] Zaika SV, Baranova II, Martyniuk TV. Features of the introduction of the component piroctone olamine to the foam base. in:10th International Pharmaceutical Conference, Science and Practice 2019. (p. 111). Lithuanian University of Health Sciences.
[20] M. Shakibaie, M. Haghiri, M. Jafari, S. Amirpour-Rostami, A. Ameri, H. Forootanfar, M. Mehrabani, Preparation and evaluation of the effect of F e3 O 4@ piroctone olamine magnetic nanoparticles on matrix metalloproteinase-2: a preliminary in vitro study, Biotechnol. Appl. Biochem. 61 (6) (2014) 676–682.
[21] M.R. Khorramizadeh, Z. Esmail-Nazari, Z. Zarei-Ghaane, M. Shakibaie, K. Mollazadeh-Moghaddam, M. Iranshahi, A.R. Shahverdi, Umbelliprenin-coated Fe3O4 magnetite nanoparticles: antiproliferation evaluation on human Fibrosarcoma cell line (HT-1080), Mater. Sci. Eng. C 30 (7) (2010) 1038–1042.
[22] M. Mostafavi, I. Sharifi, S. Farajzadeh, P. Khazaeli, H. Sharifi, E. Pourseyedi, S. Kakooei, M. Bamorovat, A. Keyhani, M.H. Parizi, A. Khosravi, Niosomal formulation of amphotericin B alone and in combination with glucantime: in vitro and in vivo leishmanicidal effects, Biomed. Pharmacother. 116 (2019), 108942.
[23] H. Mahmoudvand, F. Kheirandish, S.R. Mirbadie, M.H. Kayedi, T.R. RIABI, A. A. Ghasemi, M. Bamorovat, I. Sharifi, The potential use of methotrexate in the treatment of cutaneous leishmaniasis: in vitro assays against sensitive and meglumine antimoniate-resistant strains of Leishmania tropica, Iran. J. Parasitol. 12 (3) (2017) 339.
[24] H. Mahmoudvand, E. Saedi Dezaki, B. Ezatpour, I. Sharifi, F. Kheirandish, M. Rashidipour, In vitro and in vivo antileishmanial activities of Pistacia vera essential oil, Planta Med. 82 (2016) 279–284.
[25] B. Ezatpour, E. Saedi Dezaki, H. Mahmoudvand, M. Azadpour, F. Ezzatkhah, In vitro and in vivo antileishmanial effects of pistacia khinjuk against leishmania tropica and leishmania major, Evid. Based Complement. Altern. Med. 2015 (2015) 1–6, https://doi.org/10.1155/2015/149707. Epub 2015 Feb 28. PMID: 25815025; PMCID: PMC4359887.
[26] Q. Gan, X. Lu, Y. Yuan, J. Qian, H. Zhou, X. Lu, J. Shi, C. Liu, A magnetic, reversible pH-responsive nanogated ensemble based on Fe3O4 nanoparticles-capped mesoporous silica, Biomaterials 32 (7) (2011) 1932–1942.
[27] Y. Wei, G. Yin, C. Ma, Z. Huang, X. Chen, X. Liao, Y. Yao, H. Yin, Synthesis and cellular compatibility of biomineralized Fe3O4 nanoparticles in tumor cells targeting peptides, Colloids Surf. B Biointerfaces 107 (2013) 180–188.
[28] A. Nafari, K. Cheraghipour, M. Sepahvand, G. Shahrokhi, E. Gabal, H. Mahmoudvand, Nanoparticles: new agents toward treatment of leishmaniasis, Parasite Epidemiol. Control 10 (2020), e00156.
[29] S. Laurent, D. Forge, M. Port, A. Roch, C. Robic, L. Vander Elst, R.N. Muller, Magnetic iron oxide nanoparticles: synthesis, stabilization, vectorization, physicochemical characterizations, and biological applications, Chem. Rev. 108 (6) (2008) 2064–2110.
[30] R. Dorostkar, M. Ghalavand, A. Nazarizadeh, M. Tat, M.S. Hashemzadeh, Anthelmintic effects of zinc oxide and iron oxide nanoparticles against Toxocara vitulorum, Int. Nano Lett. 7 (2) (2017) 157–164.
[31] D. Kannan, N. Yadav, S. Ahmad, P. Namdev, S. Bhattacharjee, B. Lochab, S. Singh, Pre-clinical study of iron oxide nanoparticles fortified artesunate for efficient targeting of malarial parasite, EBioMedicine 45 (2019) 261–277.

[32] D. Zanella, E. Bossi, R. Gornati, C. Bastos, N. Faria, G. Bernardini, Iron oxide nanoparticles can cross plasma membranes, Sci. Rep. 7 (1) (2017), 11413.
[33] P. Holzmuller, D. Sereno, M. Cavaleyra, I. Mangot, S. Daulouede, P. Vincendeau, J. L. Lemesre, Nitric oxide-mediated proteasome-dependent oligonucleosomal DNA fragmentation in Leishmania amazonensis amastigotes, Infect. Immun. 70 (7) (2002) 3727–3735.
[34] R. De Lima, J.L. de Oliveira, A. Ludescher, M.M. Molina, R. Itri, A.B. Seabra, P. S. Haddad, Nitric Oxide Releasing iron Oxide Magnetic Nanoparticles for Biomedical Applications: Cell Viability, Apoptosis and Cell Death Evaluations, in: InJournal of Physics: Conference Series, Vol. 429, IOP Publishing, 2013.
[35] A.B. Seabra, P.S. Haddad, M.M. Molina, R. Itri, M.G. de Oliveira, Nitric oxide (NO) releasing-superparamagnetic iron oxide nanoparticles for biomedical applications, Nitric Oxide 27 (2012) S38.
[36] F.M. do Couto, S.C. do Nascimento, S.F. Júnior, V.K. da Silva, A.F. Leal, R.P. Neves, Antifungal activity of the piroctone olamine in experimental intra-abdominal candidiasis, SpringerPlus 5 (1) (2016) 468.
[37] S. Zhang, S. Wu, Y. Shen, Y. Xiao, L. Gao, S. Shi, Cytotoxicity studies of Fe3O4 nanoparticles in chicken macrophage cells, R. Soc. Open Sci. 7 (4) (2020), 191561.
[38] S. Patel, S. Jana, R. Chetty, S. Thakore, M. Singh, R. Devkar, Toxicity evaluation of magnetic iron oxide nanoparticles reveals neuronal loss in chicken embryo, Drug Chem. Toxicol. 42 (1) (2019) 1–8.
[39] M. Gong, H. Yang, S. Zhang, Y. Yang, D. Zhang, Y. Qi, L. Zou, Superparamagnetic core/shell GoldMag nanoparticles: size, concentration-and time-dependent cellular nanotoxicity on human umbilical vein endothelial cells and the suitable conditions for magnetic resonance imaging, J. Nanobiotechnol. 13 (1) (2015) 1–6.